OPEN ACCESS

Klimarealistene
P.O. Box 33,
3901 Porsgrunn
Norway
ISSN: 2703-9072

Correspondence:
harde@hsu-hh.de

Vol. 3.5 (2023)

pp. 445-462

Model-Experiment of the Greenhouse Effect

Michael Schnell[1], *Hermann Harde* [2]

[1]*Ex Academy of Science, Berlin, Germany*

[2]*Helmut-Schmidt-University, Hamburg, Germany*

Abstract

Radiation exchange of infrared-active gases with their environment is the basis of the atmospheric greenhouse effect (GHE). While the theoretical principles for the energy and heat exchange by infrared radiation were already refined at the end of the penultimate and beginning of the last century, experimental verifications in the laboratory showed quite contradictory results, on the one hand excluding any influence of greenhouse gases, on the other hand indicating a significantly greater impact than theoretically expected.

This study presents a simple experimental set-up, by which the infrared active gases are replaced by a broadband absorber and emitter plate in a Styrofoam hollow cylinder and by which the principles of the GHE can be demonstrated. In particular, we show that the temperature of a heated body depends on the infrared radiation of its colder surrounding and does not contradict physical laws.

Parallel heat fluxes in form of heat conduction and radiation with their mutual influence are extensively investigated, and it is shown, when the inside of the set-up is coated with an aluminum foil, up to 73% of the supplied power to a heated plate is dissipated through infrared radiation. Transferring these relationships to the heat transport in the atmosphere suggests that the CO_2 greenhouse effect not only depends on its concentration, but also on the mechanical heat flows, mainly evaporation.

Keywords: Greenhouse effect; back-radiation; radiation exchange, heat conduction

Submitted 2023-11-06, Accepted 2023-12-10; https://doi.org/10.53234/scc202310/27

1. Introduction

The so-called atmospheric greenhouse-effect (GHE) is largely controlled by the energy transfer processes in the atmosphere. While convection and heat conduction are easy to understand, the third form of energy transport, infrared (IR) radiation, is more difficult to convey. In particular, quite controversially disputed is the thesis that a heated body can further be heated up by the radiation of a colder body or gas. This is seen as a violation of the second law of thermodynamics, although Clausius [1] as one of the inventors of this law never questioned a mutual exchange of heat by radiation.

Nevertheless, a refutation of the GHE was deduced from some laboratory experiments, which demonstrated that in a compartment with a non-transparent window for IR-radiation or filled with carbon dioxide (CO_2), this gives no different temperature compared to a housing with transparent window and without CO_2 (Wood [2]; Allmendinger [3]; Nahle [4]; Seim & Olsen [5, 6]). On the other hand, there exist some deceptive demonstrations in the Internet, partially with a temperature incline of more than 10°C (e.g., v. Ditfurth [7]), which, however, have to be explained as a CO_2 stratification effect and not as GHE (Schnell [8]). Also, an unreproducible video experiment is spreading awareness for a climate crisis (Al Gore [9]), which meanwhile has also been falsified

by several revisions (Watts [10]; Solheim [11]).

It is fundamentally problematic trying to refute or prove the GHE based on just a single temperature measurement. This overlooks the fact that a higher temperature in a compartment - as in a real greenhouse - is mainly caused by suppressed convection and not by radiation exchange (Wood [2]). At best it can be shown that CO_2 is an IR-active gas that absorbs IR-radiation. The actual GHE, however, is the result of a temperature gradient in the atmosphere. For further explanations on the theory and experimental studies of the greenhouse gases CO_2, methane and nitrous oxide (with a similar experimental setup as described here) see Harde & Schnell [12].

To shed some light on this confusion, we present here some principal investigations to show what is really important when simulating the GHE in the laboratory. In Section 2 we refer to the basics of energy transport by IR-radiation and what measures have to be taken, to avoid or to determine the individual fractions of competing heat flows.

The experimental setup that is comparatively easy to implement, is explained in Section 3. It is aimed at interested people who want to demonstrate the GHE by simple means. It also addresses sceptics, who can check their reservations using the experimentally derived data.

Section 4 presents measurements of the radiation exchange between a cooler and a warmer plate, in particular the back-radiation on the heated plate. In Section 5 is the GHE simulated by placing an intermediate absorber-emitter plate between the cooled and heated plate and measuring the temperature increase of the warm plate.

To clarify what amount of heat is transferred by conductivity and by radiation, the heat losses of the set-up are investigated in detail in Section 6, and finally it is shown in Section 7 that, depending on the internal wall of the radiation channel, up to 73 % of the supplied heating power to the warm plate can be dissipated through infrared radiation.

2. Some Basics of the Radiation Exchange

Calculating the energy, dissipated from a body by IR radiation, can be complicated, if more than two bodies with different geometries and emissivities are involved in the radiation exchange. In practice, however, the calculations can be simplified with sufficient accuracy by making certain assumptions.

Ideally, for two black bodies with an emissivity $\varepsilon = 1$ and temperatures T_W and T_C, the net radiation balance ΔS_{WC} is the difference of the IR radiation between two plane-parallel, closely opposed surfaces A, with $\sigma = 5.67 \cdot 10^{-8}$ W /(m^2·K^4) as the Stefan-Boltzmann constant[1]:

$$\Delta S_{WC} = S_{BW}(T_W) - S_{BC}(T_C) = \sigma \cdot A \cdot T_W^4 - \sigma \cdot A \cdot T_C^4 = \sigma \cdot A \cdot (T_W^4 - T_C^4)\,. \quad (1)$$

Real bodies do not completely absorb the incident radiation, but rather reflect part of the radiation, which reduces the radiation balance ΔS_{WC} through reflection. From laboratory experiments Stefan [13] empirically derived the radiation balance of reflecting surfaces, which is the precursor of the well-known Stefan-Boltzmann law [14]:

$$\Delta S_{WC} = \sigma \cdot E \cdot A \cdot (T_W^4 - T_C^4)\,. \quad (2)$$

The radiation exchange efficiency E of plane-parallel surfaces is calculated from the emissivities ε_W and ε_C of the warm and cold plates as:

$$E = \left(\frac{1}{\varepsilon_w} + \frac{1}{\varepsilon_c} - 1\right)^{-1}. \quad (3)$$

[1] S_B stands for the radiation power of a body as a function of its temperature according to Stefan-Boltzmann with the additional subscripts indicating the location of this emission (Fig. 2).

For blackened, rough surfaces with emissivities $\varepsilon_{W,C} = 1$, $E = 1$, and (2) changes to (1).

A transfer of radiation and thus power between two bodies is always characterized by radiation and back-radiation. In order to replicate this process experimentally, two surfaces of different temperatures are required, which should be positioned at short distance and, if possible, parallel to each other for optimal radiation exchange.

Dulong & Petit [15] were able to realize a quite smart arrangement for the radiation exchange, when studying the cooling rate of a thermometer, heated to 200 °C in an evacuated copper vessel. The vacuum excludes mechanical heat flows and the concentrically arranged surfaces enable unhindered exchange without contact of the IR radiation with other surfaces (Fig.1).

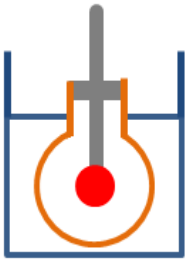

Figure 1: Set-up of the Dulong-Petit experiment.

Experimental set-ups that are easier to implement, consist of two parallel plates, which oppose each other in an elongated compartment at normal pressure, where one plate can be heated and the other cooled. The compartment enables a radiation exchange between the two plates in form of a radiation channel that directs the IR radiation from one plate to the other through multiple reflections. Due to the size and inner surface of the housing (also as potential container for IR-active gases) total reflection is excluded, while part of the radiation is absorbed by the container walls and dissipated as heat to the outside or returned to the original plate by re-emission. In such a radiation channel, there are unavoidable transmission losses, so that less heat than expected by (1), is transferred by IR radiation. This is taken into account by a transfer factor $f_T < 1$.

In previous experiments on the GHE with a similar experimental setup, a transfer factor of $f_T = 0.75$ was found. This shows that despite a larger plate distance, up to 75 % of the diffusely emitted radiation can be predominantly reflected and directed to the other plate (Harde & Schnell [12]).

This article presents a simple experimental setup for investigating the joint heat transport through heat conduction and infrared radiation. In this way, the basics of the greenhouse effect can be presented in a particularly retraceable way. However, also complex studies on the propagation and superposition of parallel heat flows can be performed, which can simulate the competing heat transport in the atmosphere and the only incompletely understood role of clouds. Parallel heat flows such as convection and evaporation reduce the radiation transport and thus the greenhouse effect of the IR-active gases, as reflected by different influences in dry or wet areas.

3. Experimental Set-Up

Fig. 2 shows the schematic of the experimental set-up, a vertical hollow cylinder made of Styrofoam, which is located in the laboratory with a constant room temperature T_R (for technical details, see Appendix). The apparatus, designed as a modular set-up, can be easily converted and therefore be used for different experiments.

The temperature T_W and the heating power H_W of the warm plate P_W give the most important information for an investigation. With these data, the back-radiation and the greenhouse effect can be determined, but also the parallel heat flows via conduction and radiation can be tracked and quantified.

The circular ring P_S (sensor plate) plays a special role. This unheated surface is a sensor for back-radiation and horizontal heat propagation, but also takes part in the radiation exchange with the cooled plate and must be taken into account when analysing and evaluating the heat flows.

Additional temperature sensors along the radiation channel are recording the mechanical heat flows at the respective positions. At the bottom the radiation channel contains the cooled plate, either with a blackened (P_C) or polished (P_{CP}) surface (Appendix, Fig. 9). Its temperature is 1°C colder than the room temperature T_R. When starting an experiment, all other temperature sensors are approximately at room temperature, while the warm plate P_W and also the sensor plate P_S in the upper position of the radiation channel will attain significantly higher temperatures after switching on the heating. This results in air stratification with a temperature gradient from top to bottom, which excludes convection as a possible heat transport. A digital laboratory power supply with a constant voltage of 4.0 volts is used for the electrical heating of the plate P_W, supplying a power of H_W = 1.2 W.

The greenhouse effect is simulated by placing an additional blackened aluminum disk P_I into the radiation channel. Such an intermediate plate, like greenhouse gases, can absorb infrared radiation and re-emit it according to its own temperature. This property is the core of the greenhouse theory, which leads to an increase in the temperature T_W of the warm plate P_W. This plate acts as heat source and sensor at the same time.

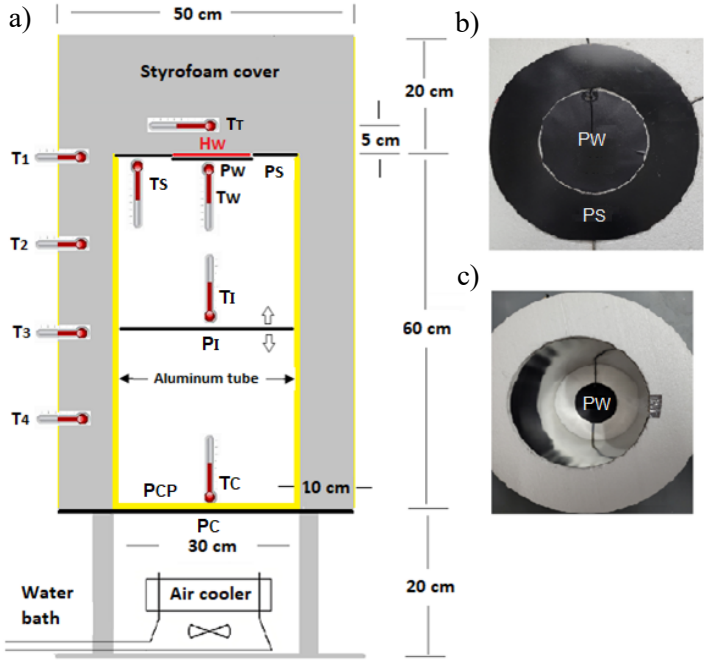

Figure 2: a) Experimental set-up of the Styrofoam radiation channel with internal aluminum tube, temperature sensors T *and plates* P *(subscripts: T-top, W-warm, S-sensor, I-intermediate, C-cold, CP-cold polished). b) Top of radiation channel with warm plate* P_W *and sensor plate* P_S. *c) Radiation channel with polished aluminum tube before installing the sensor plate* P_S.

4. Evidence of Back-Radiation

The P_W and P_S plate release part of their heat through radiation exchange with their surroundings. While the IR-emission of these plates is clearly defined by their temperatures T_W and T_S and their emissivities $\varepsilon_{W,S}$ = 1, the radiation from the environment, the so-called back-radiation, is inherently much more complex. This radiation results from a superposition of emissions and reflections that emanate from the cooled plate and the channel wall of the hollow cylinder. This will be demonstrated for the base plate by varying its surface and temperature.

Even the word back-radiation is questioned by critics of the greenhouse effect, who claim that the laws of physics do not allow such radiation or that an observation according to (1) or (2) would only be possible in vacuum.

The IR emission of the cold plate P_C is undoubtedly self-sufficient radiation, which, according to the Stefan-Boltzmann law, only depends on the plate temperature T_C and the emissivity ε_C:

$$S_{BC}(T_C) = \sigma \cdot \varepsilon_C \cdot A_C \cdot T_C^4 \,. \qquad (4)$$

Fig. 3 shows two examples illustrating how the temperature of the constantly heated plate P_W is influenced by the back-radiation[2]. After having reached thermal equilibrium (~ 100 minutes), the black coated base plate P_C is further cooled down from 17 to 11 °C (Fig. 3a). Due to (2) the radiation exchange between the plates increases and the temperature T_W decreases accordingly. In Fig. 3b, the base plate is replaced by a polished disc P_{CP} under otherwise same conditions as in Fig. 3a. Owing to the significantly reduced absorptivity, respectively emissivity (α_C resp. ε_C), the radiation transfer is reduced accordingly and the temperature T_W increases till thermal equilibrium is established. In contrast to the blackened plate, there is hardly any reaction to T_W, when the P_{CP} plate cools down. This is explained by the fact that with reduced emissivity, the reflectivity $r_C = 1 - \varepsilon_C$ increases and the emission from the cooled plate is largely replaced by the reflected radiation from the warm plate. Their radiation losses are reduced accordingly[3]. A change in thermal conductivity, as a possible cause of these effects, can be ruled out in these experiments (see Sec. 6).

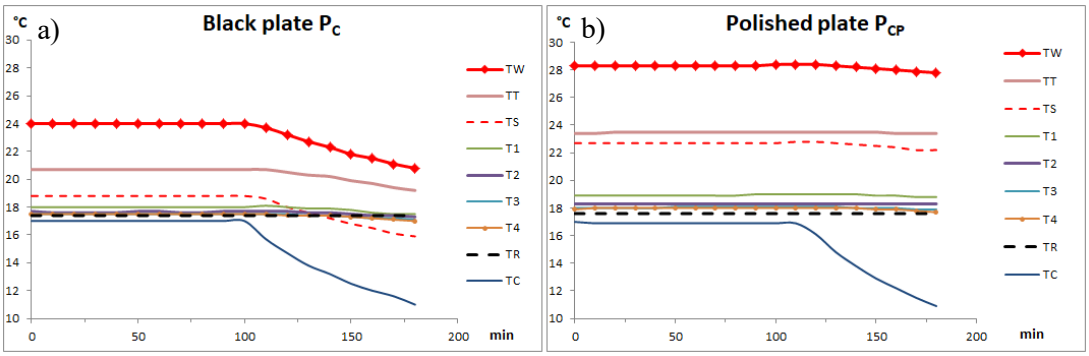

Figure 3: Impact of the back-radiation on the temperature T_W of the warm plate P_W*, a) with blackened plate* P_C *and b) with polished plate* P_{CP}.

The heat loss of a body to its colder environment, in this case the heated plate, is determined by the temperature difference ΔT_W with and without heating[4] as:

$$\Delta T_W = T_W(H_W) - T_W(0) = \vartheta_T \cdot H_W \,. \qquad (5)$$

H_W is the dissipated heat, which in equilibrium is equal to the heating power supplied, and ϑ_T (°C/W) represents the total thermal resistance of the experimental setup, which includes all heat flows. According to (5), even with a constant supply of heat, a body experiences a temperature increase when the thermal resistance ϑ_T increases. In the same way, the greenhouse effect can be described by a respective resistance ϑ_G (Section 5).

Therefore, the results are in full agreement with (1) and (2), according to which the temperature T_W of a heated body also depends on the intensity of the back-radiation of its surrounding, even when the surrounding is colder than the considered body.

---

[2] In analogy to the back-radiated and back-scattered radiation in the atmosphere we use this term here, too.

[3] The radiation exchange E explicitly takes into account that radiation is not only absorbed by surfaces, but also reflected.

[4] ΔT_W is the temperature increase of plate P_W from a lower to a higher thermal equilibrium, which establishes after switching on the heating H_W (Fig. 4).

Transferred to the Earth this means, the Earth's surface is heating up stronger, when the intensity of the atmospheric back-radiation increases. Back-radiation is not a privilege of greenhouse gases, because aerosols or clouds also produce infrared radiation in the atmosphere. At the same temperature, their radiation intensity would even be higher than that of the gases, since all IR wavelengths of a Planckian radiator are contributing to this radiation. The effect of low clouds, which is noticeable at mild night temperatures, is particularly impressive. In comparison, CO_2 has only a small influence and cannot come close to keeping up with clouds, as shown by the strong nighttime cooling in arid deserts despite high daytime temperatures (and despite rising CO_2 concentrations).

5. Simulation of the Greenhouse Effect

When modeling the greenhouse effect, the question is, what effects an unheated IR-active body in the radiation channel on the heat transport. When planning the corresponding experiment, it is important to ensure that such a body must have an absorption coefficient ε close to 1 and a high thermal conductivity λ, in order not to build up an additional thermal resistance in the radiation channel. A 0.5 mm thin aluminum disk, blackened on both sides, called as intermediate plate P_I, meets both conditions (Fig. 2a). A thin layer thickness and thermal conductivity λ_{Al} = 220 W/(m·°C) ensure a high heat flow in the aluminum disc.

In the radiation channel, disk P_I interrupts the radiation exchange through an absorption-emission cycle, whereby the energy supplied, is released again on both sides by infrared radiation. This process, in principle, corresponds to the effect of greenhouse gases in the atmosphere, with the difference that in the black disk all available wavelengths of a Planck radiator are affected by the absorption-emission interruption. In this model experiment, the cooled plate P_C is the energy sink, the place where the net energy transmitted by IR radiation is dissipated.

The model experiment can also be viewed as a simulation of the impact of clouds on the radiation exchange. In this sense, the disk P_I simulates a complete cloud cover and P_W the earth's surface.

Another sensor on the disk P_I provides information about the temperature T_I that occurs at this location, which would correspond to the temperature of the gases or clouds.

By definition, the measure of the greenhouse effect is the temperature increase ΔT_G of the warm plate compared to a measurement without a plate P_I but the same heating H_W. The respective resistance can be defined as $\vartheta_G = \Delta\vartheta_T = \vartheta_T$ (with disc) - ϑ_T (no disc). In three experimental setups, that differ only in the distance between the disk P_I and the warm plate, the existence of this plate in the beam path causes well observable temperature differences of up to 2.0 °C (Table 1).

Table 1: Greenhouse effect of a blackened disc for a constant heating output H_W = 1.2 W.

Intermediate plate P_I distance to P_W (cm)	T_W (0) °C	$T_W(H_W)$ °C	T_I °C	ΔT_W °C	ΔT_G °C	H_W W	ϑ_T °C/W	ϑ_G °C/W
5	16.9	26.1	19.8	9.2	2.0	1.20	7.7	1.7
30	16.9	25.7	19.0	8.8	1.6	1.20	7.4	1.4
55	16.9	25.3	18.5	8.4	1.2	1.20	7.0	1.0
no disc	16.8	24.0	-	7.2	-	1.20	6.0	-

For the plates P_W and P_S, the source of the back-radiation is no longer plate P_C, but the warmer plate P_I with the temperature T_I (Fig. 4, Dashed Red). This is recorded accordingly as an increase in the temperature T_W (Red) and T_S (Light Green). For comparison are shown the temperatures T_W and T_S without disk P_I (Blue lines). Once again, this confirms what was already proven in Sec. 4:

The temperature of a heated body clearly depends on the intensity of the back-radiation of its surrounding, even when this is colder, and it experiences an increase ΔT_G when ϑ_T increases.

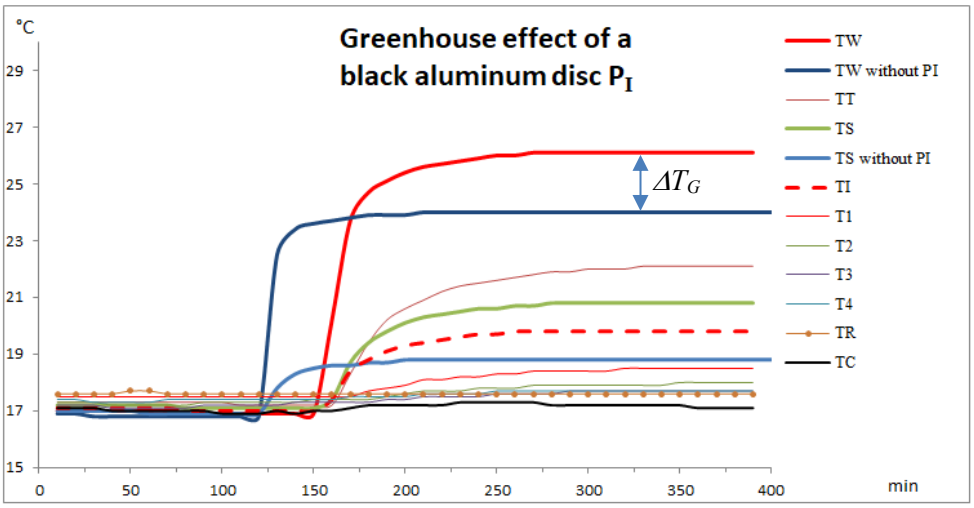

Figure 4: Temperatures in the radiation channel with intermediate plate P_I *(5 cm below plate* P_W*) before and after switching on the heating* H_W*. For comparison, the temperatures* T_W *and* T_S *without disk* P_I *(blue lines).*

The simulated greenhouse effect is also reflected in the trend of the thermal resistance ϑ_G, which characterizes this impact and which increases, the closer disk P_I comes to the warm plates P_W and P_S, and thus causes a temperature increase of T_W in analogy to (5) (Table 1).

Applied to the atmosphere this means, low clouds with their comparatively high temperatures and broad emission generate such a strong back-radiation that contributions from greenhouse gases are strongly masked and only show a minor effect. Accordingly, under a higher cloud cover with lower temperature, the fraction of IR-active gases to the GHE is increasing (Harde [16]).

6. Heat Losses at Radiation Transfer

In order to check how far the above measurements really reveal an exchange of radiation between the plates and not heat conduction, some additional investigations are required. For this purpose, the disk P_I is again removed.

6.1 Preliminary Theoretical Considerations

Without external heating, all surfaces in the radiation channel have approximately the room temperature (Fig. 4, up to minute 120). When energy is supplied to the plate P_W in form of a constant electrical heating power H_W, its temperature increases until an equilibrium of supplied and dissipated power is reached.

This power is dissipated through radiation exchange ΔS_{BW} between the heated and cold plate, a parallel exchange ΔS_{BS} between the unheated sensor plate and the cold plate, as well as a mechanical heat flow J_Q to the laboratory room with temperature T_R (Fig. 5a).

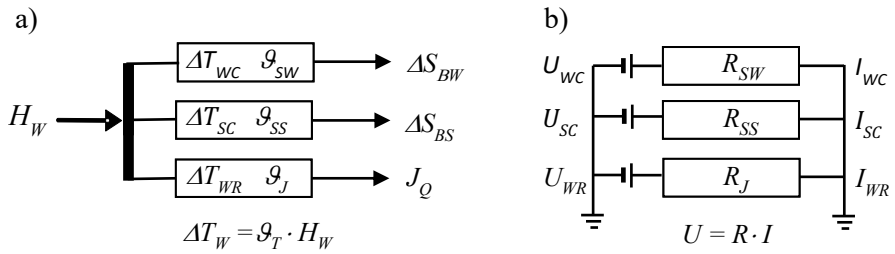

Figure 5: a) Heat fluxes of radiation and conductivity, b) equivalent electrical circuit diagram.

However, these heat flows only occur when there is a temperature difference to their surrounding inside and outside the experimental set-up. For ΔS_{BW} and ΔS_{BS} these are the differences ΔT_{WC} and ΔT_{SC} to the cooled plate, for J_Q it is the difference ΔT_{WR} to the room air. They form the drive for these flows and, in equilibrium, are also determined by the power H_W and these flows.

For smaller powers and corresponding temperature changes the net radiation exchange can be expressed in good approximation by differentiating (1):

$$\begin{aligned} \Delta S_{Bi} &= \sigma \cdot \left(\varepsilon_i \cdot A_i \cdot T_i^4 - \varepsilon_C \cdot A_C \cdot T_C^4\right) \\ &\approx 4 \cdot \sigma \cdot \varepsilon_i \cdot A_i \cdot T_i^3 \cdot \Delta T_{iC} = 4\frac{S_{Bi}(T_i)}{T_i}\Delta T_{iC}\,; \;\; i = w,s \\ &= q_{Si} \cdot \Delta T_{iC} = \frac{1}{\vartheta_{Si}} \cdot \Delta T_{iC}\,, \end{aligned} \tag{6a}$$

with

$$q_{Si} = \frac{1}{\vartheta_{Si}} = 4\frac{S_{Bi}(T_i)}{T_i} \tag{6b}$$

as the specific heat transfer by radiation and ϑ_{Si} as the radiation resistance.

Since due to multiple scattering and reflection losses occur in a radiation channel with side walls, compared to the theoretically expected radiation exchange according to (6), this must be taken into account by a transfer factor f_T. The total radiation balance ΔS_{BT}, which is only of further interest, is therefore given as:

$$\Delta S_{BT} = f_T \cdot (\Delta S_{BW} + \Delta S_{BS}) = \frac{1}{\vartheta_{ST}} \cdot \Delta T_{WS}\,. \tag{6c}$$

ϑ_{ST} is the total radiation resistance and ΔT_{WS} a weighted temperature difference of the two top plates to the cold plate.

According to Fourier, the mechanical heat flow J_Q can be calculated in good approximation from the thermal conductivity λ_{St} of the Styrofoam insulation, its thickness d and its surface A_{St} as:

$$\begin{aligned} J_Q &= \lambda_{St} \cdot \frac{A_{St}}{d}\Delta T_{WR} \\ &= q_J \cdot \Delta T_{WR} = \frac{1}{\vartheta_J} \cdot \Delta T_{WR} \end{aligned} \tag{7a}$$

with

$$q_J = \frac{1}{\vartheta_J} = \lambda_{St} \cdot \frac{A_{St}}{d} \tag{7b}$$

as conductivity and ϑ_J as resistance of the mechanical heat flow.

Since in thermal equilibrium not more heat can be dissipated than supplied, the heat flows add up to the electric heating H_W with

$$H_W = \Delta S_{BT} + J_Q\,. \tag{8}$$

The addition of the heat flows can be directly compared with the parallel connection of resistors in an electrical circuit (Fig. 5b), in which the temperature differences correspond to the applied voltages and the heat fluxes correspond to the electric currents, which add up to the total current according to Kirchhoff's rule and Ohm's law.

Applied to the atmosphere, this also means: The overall balance between the Earth's surface and the atmosphere is always determined by the parallel heat transfer channels such as radiation, heat conduction, convection and evaporation. With the same total power supplied, an increase in one process has the opposite effect on the other channels.

The heat flow J_Q can be determined experimentally by the heating power H_W, when the radiation exchange is prevented by a special experimental setup, the so-called Styrofoam block, where $\Delta S_{BT} = 0$ and (8) transitions to

$$J_Q = H_W \ . \tag{9}$$

The thermal conductivity λ_{St}, thickness d and surface area A_{St} are fixed design features of the apparatus that define the thermal conduction resistance ϑ_J and, as the reciprocal, the specific heat conduction q_J. Thus, via (7) and (9), q_J can be determined from the heating H_W and the difference between the inside and outside temperature ΔT_{WR}, this for different configurations of the radiation channel, which differ in their wall lining.

For "radiation experiments", the inner Styrofoam disks are removed from the Styrofoam block to get the radiation channel. This change has no influence on the external thermal insulation, so that the competing heat flow J_Q of the hollow cylinder now can be calculated by means of the known specific heat conduction q_J according to (7) (see Section 7).

When the heat flow J_Q is known, the total radiation balance ΔS_{BT}, i.e., that part of the heating output H_W, which is dissipated by IR radiation, can also be calculated:

$$\Delta S_{BT} = H_{SB} = \ H_W - J_Q \ . \tag{10}$$

H_{SB} is the heating power H_W minus the heat flow J_Q, i.e., that part of the heating output H_W that is available for radiation exchange.

6.2 Determination of the Heat Flow J_Q in a Styrofoam Block

To determine the heat flow J_Q of the experimental set-up, the radiation exchange ΔS_{BT} must be prevented. In this case, all supplied power flows exclusively as heat flux J_Q outwards according to (7). For this measurement the aluminum tube is removed from the hollow cylinder and the exposed channel is completely filled with 12 polystyrene disks (Fig. 6).

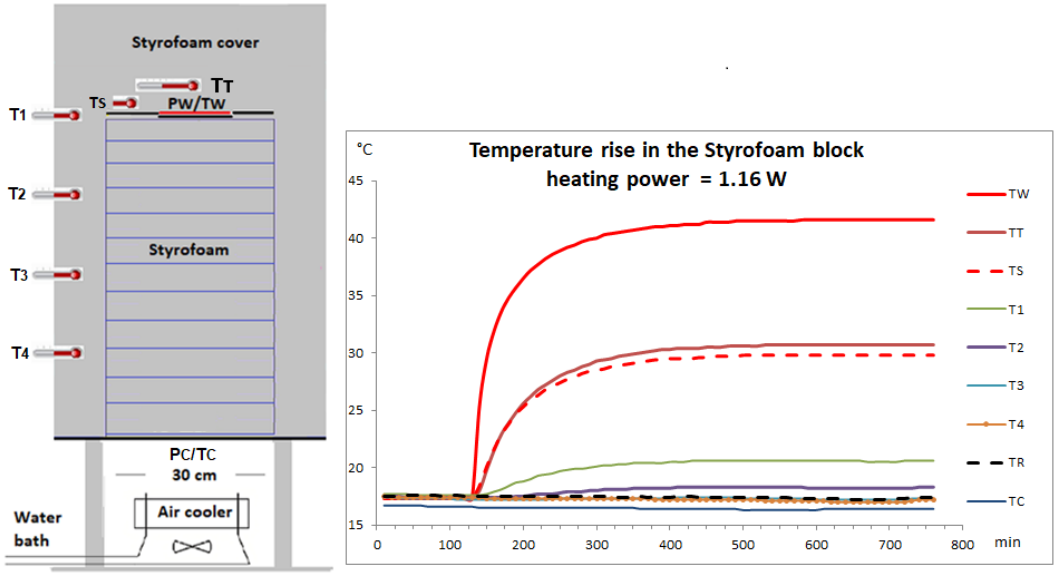

Figure 6: Determination of the insulation loss J_Q of the Styrofoam compartment.

When the heating is switched on, the plate P_W heats up to a temperature of 41.6 °C within around 500 minutes and holds this temperature for the next 200 minutes. The constant T_W temperature proves thermal equilibrium, in which heat input (H_W) and heat removal (J_Q) according to (9) are the same (Fig. 6, right).

The heat from plate P_W mainly flows outwards via the upper Styrofoam cover, as can be seen

from the temperatures T_T = 30.9 °C (Brown Line) and T_S = 29.9 °C (Red Dashed). This is in agreement with the expectation, since the warm plate P_W is located in the upper quarter of the set-up and has physical contact with the Styrofoam lid.

A downward spread towards the cold plate P_C is hindered by the simultaneous lateral heat flow, so that the temperatures of the Styrofoam wall T_1 = 20.6 °C and T_2 = 18.4 °C are only slightly higher than the room temperature T_R = 17.4 °C.

From the difference between the inside and outside temperature ΔT_{WR} and the heating output $H_W = J_Q$, the thermal resistance ϑ_J or the heat conduction q_J for mechanical heat dissipation is calculated according to (7a).

The measurements are repeated for a larger temperature range with two additional heating levels H_W = 0.66 W and H_W = 0.30 W. Only small deviations in the thermal resistance and heat conduction are found. Their averages are listed in Table 2.

Table 2: Specific resistance ϑ_J and heat conduction q_J for different configurations.

Channel wall	T_W °C	T_R °C	ΔT_{WR} °C	H_W (J_Q) W	ϑ_J °C/W	q_J W/°C
Styrofoam	41.6	17.4	24.2	1.16	20.95	0.048
Al-foil	40.5	17.6	22.9	1.15	19.98	0.050
Al-tube	38.0	17.5	20.5	1.16	17.67	0.057

The internal channel is then covered with an aluminum foil or an aluminum tube and filled again with 12 Styrofoam discs. As before, thermal resistance ϑ_J and heat conduction q_J are determined for these experimental configurations using three heating stages.

6.3 Heat Diffusion in a Styrofoam Channel

To control how far the heat conduction expands to the lower plate P_C and could overlap with the radiation transport, the lowest discs from the Styrofoam block (see Subsection 6.2) are gradually removed from the radiation channel. This creates a partial channel (BRC = bottom radiation channel) above the cold plate P_C with the variable length L_{BRC} (Fig. 7).

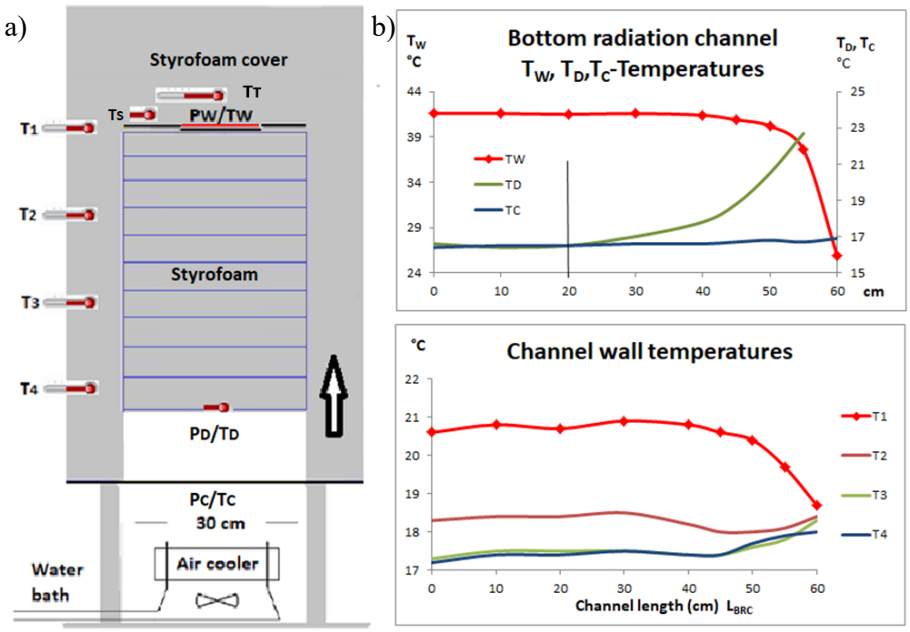

Figure 7: a) Bottom radiation channel BRC above plate P_C, b) Temperatures via channel length L_{BRC}.

For our further considerations, not the channel formed, is of interest, only the layer thickness of the Styrofoam disks still present under the warm plate P_W and the temperature T_D of the lowest Styrofoam disk[5].

As long as no heat from the plate P_W reaches the lowest Styrofoam disk, the radiation exchange between the plates P_C and P_D leads to the same temperatures $T_C = T_D$. Indeed, this is observed, when removing the first 4 Styrofoam disks (Fig. 7b). Only when additional polystyrene disks are taken away and the channel length L_{BRC} gets longer than 20 cm, the temperature T_D (Green line) is initially slightly and then significantly higher than T_C (Blue line). From these temperature measurements it can be concluded that the heat from the plate P_W flowing laterally and also downwards, is completely dissipated to the outside after around 40 cm. Mechanical heat conduction through the channel jacket to the cooled plate can therefore be ruled out, and heat conduction via air in the radiation channel plays no role, as has already been demonstrated in previous studies with noble gases of different thermal conductivities [12].

Of particular interest is the removal of the last disk (L_{BRC} = 60 cm), when radiation exchange between the plates P_W and P_C is possible. It is reflected as a significant drop of T_W by 11.7 °C (Fig. 7b, top image). This temperature effect demonstrates that heat is transported over larger distances primarily through infrared radiation and not through heat conduction.

6.4 Heat Dissipation in a Styrofoam Channel with Internal Aluminum Cladding

To optimize the radiation exchange, the radiation channel can be lined with a polished 0.5 mm thick aluminum sheet (Fig. 2, without plate P_I), which should have a positive effect on the radiation exchange (Section 7.2).

However, aluminum has a very high thermal conductivity λ_{Al} = 220 W/(m·°C), also changing the thermal conduction J_Q of the set-up. The heat conduction of a Styrofoam block with an aluminum tube increases by 19 % to q_{Al} = 0.057 W/°C, compared to the pure Styrofoam lining, and the thermal resistance drops to ϑ_J = 17.67 °C/W (Table 2).

As before, when the lowest polystyrene discs are gradually removed, a maximum spread of 40 cm below the plate P_W (Fig. 8, L_{BRC} = 20 cm) is detected. A mechanical heat flow between the P_W and P_C plates can therefore also be excluded with an internal aluminum tube (Fig. 8).

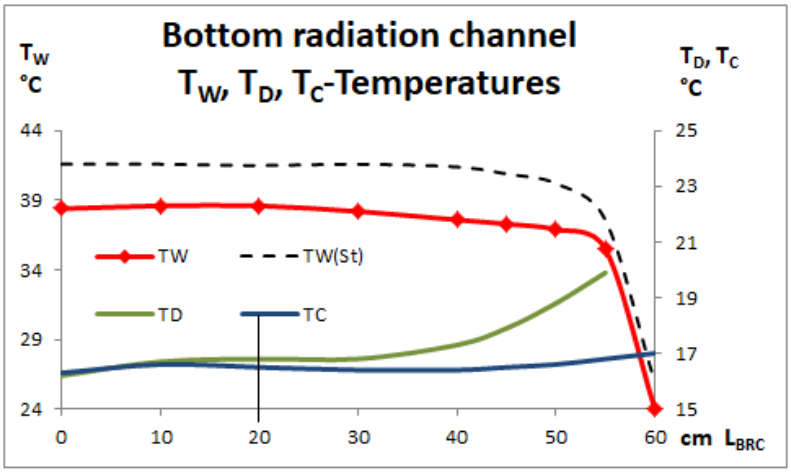

Figure 8: Heat spread towards the P_C *plate. Comparison with temperature* $T_{W(St)}$ *for the Styrofoam duct without aluminum tube (Black Dashed).*

[5] The thickness of the Styrofoam discs is 60 – L_{BRC} cm. Since the conductivity of air λ_L = 0.026 W/(m·°C) is slightly lower than that of Styrofoam with λ_{St} = 0.035 W/(m·°C), we can be sure that the new channel of length L_{BRC} does not elevate mechanical heat conduction downwards.

The only notable difference to the Styrofoam channel $T_W(St)$ is the lower T_W temperature for the same heating output, which is explained in more detail in Subsection 7.2.

The heat conduction of an aluminum layer also depends, among other things, on its layer thickness. So, it makes sense to replace the aluminum sheet by a thin aluminum foil as internal coating.

The measurements for the specific heat conduction give q_J = 0.050 W/°C, which is only slightly higher than the hollow Styrofoam cylinder with 0.048 W/°C, and thus represents a good alternative to the aluminum tube for a duct surface with a high degree of reflection (Table 2).

7. Share of Infrared Radiation to the Total Heat Dissipation

Hollow cylinders with end plates of different temperatures dissipate the released heat through both infrared radiation and heat conduction, according to (8). The ratio of the two heat flows depends on the thermal insulation, the diameter and length of the channel and in particular on its surface. The latter will be demonstrated using three examples with different surfaces in the radiation channel.

At a first glance, such an investigation is very special and should only be of interest to specialists who are thinking about experiments on the greenhouse effect. However, we have to remind on the fact that the Earth's surface also has various transport mechanisms for dissipating heat from the surface. Understanding the different heat flows and their interdependence also enables a deeper insight into the greenhouse effect and its real or perceived impact on climate change.

a) Radiation Transfer in a Styrofoam Hollow Cylinder

According to (10), with the knowledge of J_Q, the total radiation balance ΔS_{BT} is found as difference of H_W and J_Q. Table 3 shows the temperatures measured in a hollow cylinder of Styrofoam with a heating output of H_W = 1.2 W, and the share of infrared radiation of the total heat flow that is derived from this.

The calculation of the power balances starts with the mechanical flow J_Q = 0.39 W, which, according to (7a), results from the temperature difference $\Delta T_{WR} = T_W - T_R$ and the specific heat conduction q_J = 0.048 W/°C (Table 2). Based on the 1.2 W heating, 32.8 % is conducted outwards through J_Q. The power $H_{SB} = H_W - J_Q$ = 0.81 W corresponds to the radiation exchange ΔS_{BT}, which transfers the heat from the two plates P_W and P_S to the plate P_C. Accordingly, 67.2 % of the heat is dissipated directly or indirectly through infrared radiation (Table 3).

Table 3: Styrofoam hollow cylinder: Temperatures and power balance.

T_R °C	T_C °C	T_W °C	T_S °C	T_T °C	T_1 °C	T_2 °C	T_3 °C	T_4 °C
17.7	16.9	25.9	20.9	22.1	18.7	18.4	18.3	18.0
P_W/P_S m²	S_{BC} W	S_{BW} W	S_{BS} W	ΔS_{BW} W	ΔS_{BS} W	$\Delta S_{BW}+\Delta S_{BS}$ W	H_{SB} W	f_T
0.019	7.63	8.62	-	0.99	-	2.16	0.81	0.37
0.052	20.79	-	21.96	-	1.17			
H_W W	ΔT_W °C	ΔT_{WR} °C	ϑ_T °C/W	ϑ_{ST} °C/W	ϑ_J °C/W	q_J W/°C	ΔS_{BT} W	J_Q W
1.20	8.8	8.2	7.3	10.9	20.8	0.048	0.81	0.39
							67.2%	32.8%

In order to determine the radiation losses in the Styrofoam cylinder, the theoretical radiation for all three plates P_C, P_W and P_S (S_{BC}, S_{BW}, S_{BS}) is calculated according to the Stefan-Boltzmann law

for $\varepsilon = 1$ and their respective areas. The net radiation exchange between P_W and P_C or between P_S and P_C as defined by (6a), is given as ΔS_{BW} and ΔS_{BS}. The ratio $H_{SB}/(\Delta S_{BW} + \Delta S_{BS})$ defines the transmission factor f_T accordingly (6c).

It turns out that even with a simple radiation channel made of Styrofoam with a transmission factor $f_T = 37$ %, the heating power H_W is mainly (67 %) dissipated by infrared radiation from the warm plates P_W and P_S.

Due to the parallel heat flows with the resistances ϑ_{Si} ($i = w, s$) for radiation and ϑ_J for mechanical heat transport, the total resistance ϑ_T is always smaller than the individual resistances.

b) Radiation Transfer in a Styrofoam Hollow Cylinder with an Aluminum Tube

To optimize the radiation exchange, the radiation channel is lined with a polished 0.5 mm thick aluminum sheet. The IR radiation is mainly reflected on this smooth surface and less scattered or absorbed, which should reduce radiation losses in the channel and thus promote radiation exchange. Table 4 shows the temperatures and power balances that arise with a heater output H_W = 1.2 W for a radiation channel with an aluminum tube. The calculation of the energy balances is carried out as described above.

Overall, the heat dissipated by radiation is only slightly increased to 69.1 % vs. 67.2 % without the aluminum pipe. The reason is the higher heat conduction of the aluminum tube, which contributes to an increase in the heat flow J_Q and partially compensates the advantage of better reflection.

Table 4: Styrofoam hollow cylinder with aluminum tube: Temperatures and power balance.

T_R °C	T_C °C	T_W °C	T_S °C	T_T °C	T_1 °C	T_2 °C	T_3 °C	T_4 °C
17.5	17.0	24.0	18.8	20.7	17.9	17.6	17.4	17.4
P_W/P_S m^2	S_{BC} W	S_{BW} W	S_{BS} W	ΔS_{BW} W	ΔS_{BS} W	$\Delta S_{BW}+\Delta S_{BS}$ W	H_{SB} W	f_T
0.019	7.64	8.40	-	0.76	-	1.29	0.83	0.65
0.052	20.82	-	21.34	-	0.52			
H_W W	ΔT_W °C	ΔT_{WR} °C	ϑ_T °C/W	ϑ_{ST} °C/W	ϑ_J °C/W	q_J W/°C	ΔS_{BT} W	J_Q W
1.20	7.2	6.5	6.0	8.7	17.5	0.057	0.83	0.37
							69.1%	30.9%

c) Radiation Transfer in a Styrofoam Hollow Cylinder with an Aluminum Foil

An aluminum foil causes a lower specific heat conduction of $q_J = 0.050$ W/°C in the Styrofoam block compared to 0.057 W/°C for the aluminum tube (Table 2) at comparable reflection properties in the hollow cylinder. This also affects the radiation transfer ΔS_{BG}, whereby around 73 % of the H_W power is dissipated through IR radiation with an aluminum foil (Table 5).

In summary, coating the Styrofoam channel with an aluminum sheet or aluminum foil improves the reflection properties of the radiation channel, and thereby, increases significantly the transmission factor from $f_T = 0.37$ to $f_T = 0.65$ (Tables 4 and 5).

A channel without coating also shows the direct consequences for the greenhouse effect: When the radiation transport decreases (the respective resistance increases, in this case due to the lower transfer factor $f_T = 0.37$), the temperature T_W of the warm plate inclines, in this case from 24.0 °C to 25 .9 °C to overcome the bottleneck. On the other hand, when the parallel heat flow J_Q increases from 0.33 to 0.37 W (a sheet of metal dissipates more heat than an aluminum foil), the radiation

transport ΔS_{BT} must decrease from 0.88 to 0.83 W.

Table 5: Styrofoam hollow cylinder with aluminum foil: Temperatures and power balance.

T_R °C	T_C °C	T_W °C	T_S °C	T_T °C	T_1 °C	T_2 °C	T_3 °C	T_4 °C
17.5	16.9	24.0	18.9	20.8	18.2	17.9	17.6	17.4
P_W/P_S m²	S_{BC} W	S_{BW} W	S_{BS} W	ΔS_{BW} W	ΔS_{BS} W	$\Delta S_{BW}+\Delta S_{BS}$ W	H_{SB} W	f_T
0.019	7.63	8.40	-	0.77	-	1.35	0.88	0.65
0.052	20.79	-	21.37	-	0.58			
H_W W	ΔT_W °C	ΔT_{WR} °C	ϑ_T °C/W	ϑ_{ST} °C/W	ϑ_J °C/W	q_J W/°C	ΔS_{BT} W	J_Q W
1.20	7.2	6.5	6.0	8.2	20.0	0.050	0.88	0.33
							72.9%	27.1%

This finding also contributes to a deeper understanding, how parallel heat fluxes affect the CO_2 GHE. In the Earth-Atmosphere System, mechanical heat flows occur only to a small extent through heat conduction, but mainly through convection and evaporation, whereby heat is removed from the Earth's surface, in addition to radiation transport (Trenberth et al. [17]). On one side this reduces the fraction of the radiation transfer, on the other side the warming of the Earth's surface, caused by increasing greenhouse gases, simultaneously leads to increased convection and evaporation, which overall manifests itself as clear negative feedback for the GHE. Cloud cover has another significant influence on the size of the GHE, as the absorption and emission bands of the GHG are superimposed by the broadband radiation emitted by clouds. Therefore, the effect of GHG under a cloud cover can significantly be reduced (see Harde [16]).

Unfortunately, the impact of evaporation on the GHE, the influence of the cloud cover and a largely saturated water vapor feedback are not taken into account in publications to which the IPCC refers. This leads to significantly higher estimates of the equilibrium climate sensitivity *ECS* (temperature increase at doubled CO_2 concentration). So, within the Coupled Model Intercomparison Project Phase 6 (CMIP6), e.g., the climate sensitivity is specified as *ECS* = 3.78 °C (IPCC, AR6-WG1-Table7.SM.5 [18]). This is more than a factor of 5 higher than this follows from own calculations with *ECS* = 0.68 °C, when taking into account the mentioned impacts, which altogether are contributing to total negative feedback (Harde [16], [19]).

8. Conclusion

Based on the physical principles, there can be no serious doubts that an IR-active body emits infrared radiation, when its temperature is > 0 K, nor about the knowledge that energy can be transported with this radiation. Only controversially discussed is, whether infrared radiation causes warming from cold to warm. This doubt contains a misleading assumption. Thermally induced radiation exchange is not about the direction of energy transfer between two surfaces of different temperatures, which also here always occurs only from warm to cold, but rather about the net radiation balance ΔS_B, which is transferred as energy per time and what effect this has on the warmer body.

To dispel these doubts, heat propagation was studied in a hollow cylinder made of Styrofoam, which is closed at both ends with aluminum plates, so that the two plates can exchange heat through infrared radiation. The upper cover consists of a heatable plate P_W and a passive sensor ring P_S, at the other end is installed an air-cooled plate P_C. In order to demonstrate the radiation transport, the plate P_W is heated with a constant heating power H_W, and the resulting temperature

increase ΔT_W of the plate P_W is measured.

In a first demonstration experiment it is shown that the cooled plate controls the radiation exchange either through self-emission or even more effectively through reflection of the incident radiation, which explains the term "back-radiation" and its meaning.

In the next step, the greenhouse effect is simulated in a model set-up. A thin, blackened metal plate P_I is attached inside the hollow cylinder, which influences the radiation transport through an absorption-emission process, similar to IR-active gases, aerosols and clouds in the atmosphere. This hindrance for the exchange of radiation leads to a significant increase in back-radiation and thus, also to an increase in the temperature of the warm plate P_W.

This model experiment and the analog measurements with greenhouse gases (Harde & Schnell [12]) refute the thesis that such warming is not physically possible. The laws of physics apply universally; what is possible in the laboratory also applies to the atmosphere.

Since heat can be transported both by thermal conduction J_Q and by infrared radiation S_B, the focus of the study was to determine, which transport processes dominate at which location and how they influence each other.

Filling the radiation channel with Styrofoam discs leads to a Styrofoam block that dissipates the heat exclusively through heat conduction outwards, from which the specific heat conduction of the Styrofoam insulation q_J is determined, and from which the heat flux J_Q can be calculated. By gradually removing the Styrofoam discs, it can be shown that the mechanical heat flux is restricted mainly to the upper insulation and the upper channel and does not reach the lower part.

With known heat flow J_Q the radiation flux ΔS_{BT} is found as the difference to the heating output H_W (eq. 10), since at thermal equilibrium both flows add up to the supplied power H_W.

The radiation losses caused by the radiation channel are taken into account by a transfer factor f_T, which follows from the ratio of measured to theoretical radiation transport.

The radiation losses can be reduced by coating the radiation channel, either with an aluminum sheet or aluminum foil, so that up to 73 % of the heating output H_W is dissipated by infrared radiation. During these tests it was found that the aluminum foil causes a smaller heat loss J_Q than the sheet, which results in a slightly increasing radiation exchange.

Since in thermal equilibrium only as much heat can be dissipated as is supplied, any changes in the mechanical heat flows have a counterbalancing effect on the radiation balance. This also largely applies to the Earth-Atmosphere System, and thus, has a direct impact on the size of the greenhouse effect.

Still controversially discussed is, how the various IR-active components of the atmosphere interact and impact each other, and how great their respective influence is. Larger discrepancies can be found for the estimated feedbacks, which within the CMIP6 studies, e.g., give an average amplification of the basic equilibrium climate sensitivity by a factor of 3.1 and a final ECS = 3.78 °C. Other studies show negative feedback with an attenuation of 36 % and an ECS of only 0.68 °C (Harde [16], [19]; Lindzen [20]).

Funding: This research did not receive any specific grant from funding agencies in the public, commercial, or not-for-profit sectors.

Editors: S. S. Bergsmark; **Reviewers**: anonymous.

Acknowledgements

We thank the Editors and Reviewers for their comments and for continuously supporting the publication process.

Appendix

A1. Description of the Experimental Set-Up

The cylindrical compartment is made of 16 round Styrofoam plates (Ø: 50, H: 5 cm), which are available as cake dummies (Fig. 2). A hole (Ø: 30 cm) is cut out of the middle of 12 of the Styrofoam panels. These 12 plates form the 60 cm long radiation channel. The 4 remaining plates (without hole) are required for the top cover of the radiation channel (H: 20 cm). The entire construction is hold together by three threaded rods, creating a radiation channel with a Styrofoam surface. The apparatus can be converted relatively easily by loosening the screw connections. From the outside, the cylinder jacket is covered with an aluminum-coated Styrofoam wallpaper

To optimize the radiation exchange, the channel is lined with a 0.5 mm thick, highly polished aluminum plate. The aluminum plate is bent to a tube and the overlap is covered with a 5 cm aluminum tape (Fig. 2). Similarly, to further minimize heat losses, the radiation channel can be lined with an aluminum-paper foil.

The warm plate P_W (Ø: 15.5 cm H: 0.5 mm, area: 0.0189 m^2) is covered with a commercially available heating foil (Thermo TECH, polyester heating foil, self-adhesive 12 V/DC, 12 V/AC 14 W, Ø = 174 mm, the plastic edges are cut to Ø = 15.5 cm) and heated electrically. The electrical power is supplied by a digital power supply (Korad KA3005D DC 30 V, 5 A) with a resolution of 0.01 V at a constant voltage of 4.00 V, unless otherwise specified. The heating output H_W, which is calculated from the voltage and measured current, shows slight deviations, caused by the ohmic resistance of the heating foil with the temperature T_W. The sensor plate P_S (Ø: 30 cm H: 0.5 mm, area: 0.052 m^2) has a hole in the middle (Ø: 15.6 cm), which is occupied by the warm plate.

The cooled plate is a 0.5 mm thick aluminum disc (Ø: 50 cm), which can be either blackened on both sides (P_C) or polished on the inside (P_{CP}). It closes the Styrofoam hollow cylinder at the bottom (Fig. 9a).

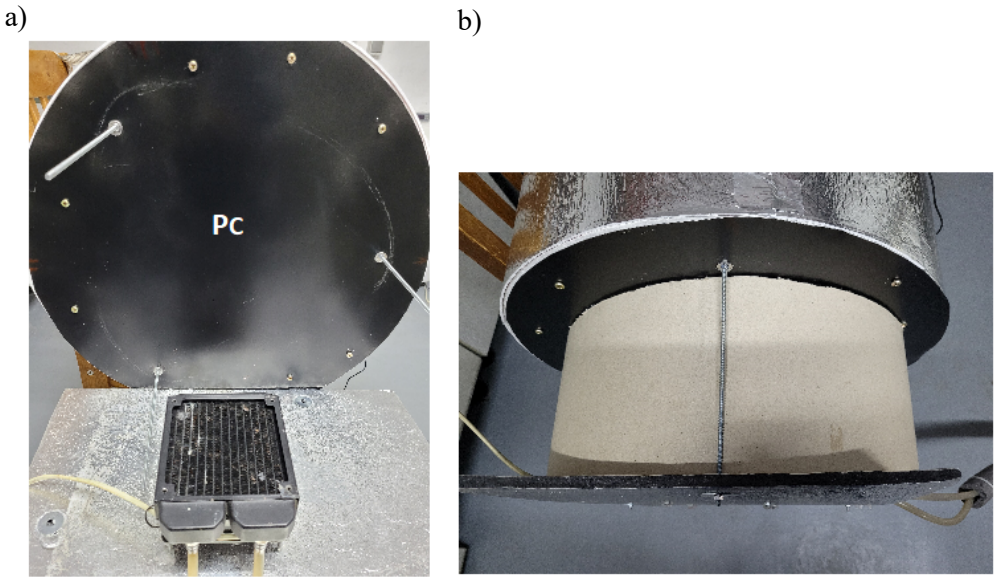

Figure 9: a) Plate P_C with air cooler b) Isolation of cooling unit.

The cold plate is cooled by a constant air flow (fan: Sunon, 120 mm Axial Panel Fan, 230 VAC, DP200A-2123XBT.GN, connected to 150 V = 8 W power consumption) and a heat exchanger (120 mm, 10 pipe, CPU cooler), so that its temperature is around 1°C below the room temperature. The fan and heat exchanger are located in an aluminum tube (H: 20 cm, Ø: 35 cm) that is wrapped with a 5 cm thick layer of polystyrene wallpaper (Fig. 9b).

The cooling water is circulated from a cool box with compressor cooling, filled with 7 liter of water. To ensure a constant water temperature, the compressor is periodically switched on and off. In the case of the cooling experiments, the compressor runs continuously.

The temperatures T_W, T_C, T_T, T_S, T_I, T_D and T_{1-4} are recorded with data loggers (Elitech, RC4HC series) at intervals of 10 minutes with a resolution of 0.1°C. An 11th data logger measures the room temperature T_R at a distance of 1 m from the apparatus at a height of 80 cm above the floor.

A constant room temperature is a prerequisite for the measurements and is set to 17.5 ± 0.2 °C by thermostating the laboratory, for which a Nanyo mobile air conditioning unit is controlled by an ESCO, ES-10 temperature controller.

References

1. R. Clausius, 1887: Die Mechanische Wärmetheorie, Band I, https://archive.org/details/diemechanischewr00clau/page/n5/mode/2up?view=theater
2. R. W. Wood, 1909: *Note on the Theory of the Greenhouse*, London, Edinborough and Dublin Philosophical Magazine, Vol. 17, pp. 319-320. https://zenodo.org/record/1430650#.Yoo9kPTP1EY
3. T. Allmendinger, 2006: *The thermal behaviour of gases under the influence of infrared-radiation,* Int. J. Phys. Sci. 11: pp. 183-205. https://academicjournals.org/journal/IJPS/article-full-text-pdf/E00ABBF60017
4. N. S. Nahle, 2011: *Repeatability of Professor Robert W. Wood's 1909 experiment on the Theory of the Greenhouse*, Biology Cabinet Online-Academic Resources and Principia Scientific International, Monterrey, N. L.
5. T. O. Seim, B. T. Olsen, 2020: *The Influence of IR Absorption and Backscatter Radiation from CO_2 on Air Temperature during Heating in a Simulated Earth/Atmosphere Experiment*, Atmospheric and Climate Sciences, 10, pp. 168-185, https://doi.org/10.4236/acs.2020.102009.
6. T. O. Seim, B. T. Olsen, 2023: *The Influence of Heat Source IR Radiation on Black-Body Heating/Cooling with Increased CO_2 Concentration*, Atmospheric and Climate Sciences, Atmospheric and Climate Sciences, 13, pp. 240-254. https://doi.org/10.4236/acs.2023.132014
7. H. v. Ditfurth, 1978*: Studio-Demonstration im ZDF*, TV-Serie "Querschnitte".
8. M. Schnell, 2020: *Die falschen Klimaexperimente*, https://www.eike-klima-energie.eu/2020/11/06/die-falschen-klima-experimente.
9. A. Gore, D. Guggenheim, 2006: *An Inconvenient Truth*, Movie, https://www.imdb.com/title/tt0497116/, Oct.21
10. A. Watts, 2011: *Replicating Al Gore's Climate 101 video experiment shows that his "high school physics" could never work as advertised*, https://wattsupwiththat.com/2011/10/18/replicating-al-gores-climate-101-video-experiment-shows-that-his-high-school-physics-could-never-work-as-advertised/?cn-reloaded=1, Oct.21
11. J.-E. Solheim, 2016: *Start des zweitägigen „Al Gore-Experiments"*, 10. Internationale Klima- und Energie-Konferenz (10. IKEK), EIKE, Berlin, https://www.eike-klima-energie.eu/2017/02/04/10-ikek-prof-em-jan-erik-solheim-start-des-zweitaegigen-al-gore-experiments/,
12. H. Harde, M. Schnell, 2022: *Verification of the Greenhouse Effect in the Laboratory*, Science of Climate Change, Vol. 1.2, pp. N4 1-32, https://doi.org/10.53234/scc202112/213.
13. J. Stefan, 1879: *Über die Beziehung zwischen der Wärmestrahlung und der Temperatur*, in: Sitzungsberichte der mathematisch-naturwissenschaftlichen Classe der kaiserlichen Akade-

mie der Wissenschaften, Bd. 79 (Wien 1879), pp. 391-428.

14. L. Boltzmann, 1884: *Ableitung des Stefan'schen Gesetzes, betreffend die Abhängigkeit der Wärmestrahlung von der Temperatur aus der electromagnetischen Lichttheorie*, Annalen der Physik und Chemie. Bd. 22, pp. 291–294, https://doi.org/10.1002/andp.18842580616.
15. P. L. Dulong, A. Petit, 1817: Annales de Chim. de Phys. VII, pp. 225 – 264 und 337 -36
16. H. Harde, 2017: *Radiation Transfer Calculations and Assessment of Global Warming by CO_2,* International Journal of Atmospheric Sciences, Volume 2017, Article ID 9251034, pp. 1-30, https://doi.org/10.1155/2017/9251034.
17. K. E. Trenberth, J. T. Fasullo, and J. Kiehl, *Earth's global energy budget*, Bulletin of the American Meteorological Society, vol. 90, no. 3, pp. 311–323, 2009.
18. Sixth Assessment Report (AR6) of the IPCC, 2021: *Summary for Policymakers*. In: Climate Change 2021: The Physical Science Basis. Contribution of Working Group I to the Sixth Assessment Report of the Intergovernmental Panel on Climate Change [Masson-Delmotte, V. et al. (eds.)]. Cambridge University Press.
19. H. Harde, 2022: *How Much CO_2 and the Sun Contribute to Global Warming: Comparison of Simulated Temperature Trends with Last Century Observations*, Science of Climate Change, Vol. 2.2, pp. 105-133, https://doi.org/10.53234/scc202206/10.
20. R. S. Lindzen, Y.-S. Choi, 2011: *On the observational determination of climate sensitivity and its implications*, Asia-Pacific Journal of Atmospheric Sciences, Vol. 47(4), pp. 377–390, https://doi.org/10.1007/s13143-011-0023-x